HHS Public Access

Author manuscript

*Am J Med Genet A*. Author manuscript; available in PMC 2024 November 01.

Published in final edited form as:

*Am J Med Genet A*. 2023 November ; 191(11): 2757–2767. doi:10.1002/ajmg.a.63363.

# Novel association of Dandy-Walker malformation with *CAPN15* variants expands the phenotype of oculogastrointestinal neurodevelopmental syndrome

**M. Makenzie Beaman**[1,2], **Lucia Guidugli**[3], **Monia Hammer**[3], **Chelsea Barrows**[3,4], **Anne Gregor**[4,5], **Sangmoon Lee**[3,4], **Kristen L. Deak**[6], **Marie T. McDonald**[1], **Courtney Jensen**[7], **Maha S. Zaki**[8], **Amira T. Masri**[9], **Charlotte A. Hobbs**[3], **Joseph G. Gleeson**[3,4], **Jennifer L. Cohen**[1]

[1]Department of Pediatrics, Division of Medical Genetics, Duke University, Durham, NC, 27710, USA

[2]Medical Scientist Training Program, Duke University, Durham, NC, 27705, USA

[3]Rady Children's Institute for Genomic Medicine, Rady Children's Hospital, San Diego, CA, 92123, USA

[4]Laboratory for Pediatric Brain Disease, University of California San Diego, La Jolla, CA, 92093 USA

[5]Department of Human Genetics, Inselspital Bern, University of Bern, Bern 3010, Switzerland

[6]Department of Pathology, Duke University, Durham, NC 27710, USA

[7]Children's Services, Duke University Health Center, Duke University, Durham, NC 27710, USA

[8]Clinical Genetics Department, Human Genetics and Genome Research Institute, National Research Centre, Department of Clinical Genetics, Cairo, 12622, Egypt

[9]University of Jordan, Department of Pediatrics, Division of Child Neurology, Amman, 11942, Jordan

## Abstract

*correspondence: jennifer.l.cohen@duke.edu.

Author Contributions

M. Makenzie Beaman: formal analysis, writing – original draft, writing – review and editing. Lucia Guidugli: formal analysis. Monia Hammer: formal analysis. Chelsea Barrows – project administration. Anne Gregor: experimental design, formal analysis, clinical evaluation. Sangmoon Lee: experimental design, formal analysis. Kristen L. Deak: formal analysis. Marie T. McDonald: clinical evaluation. Courtney Jensen: clinical evaluation. Maha S. Zaki: clinical evaluation. Amira T. Masri: clinical evaluation. Charlotte Hobbs: project administration, funding acquisition. Joe G. Gleeson: project administration, funding acquisition, experimental design. Jennifer L. Cohen: project administration, funding acquisition, writing – original draft, writing – review and editing.

Conflict of Interest Disclosure

The authors have no conflicts of interest to report.

Ethics Approval Statement

All components of this study were performed in accordance with institutional standards and appropriate institutional review board approval.

Patient Consent Statement

All participants in the study provided written informed consent in accordance with the institutional review boards at Duke University and University of California, San Diego. All participants provided consent for publication of deidentified clinical information and genome sequence data.

Oculogastrointestinal neurodevelopmental syndrome has been described in seven previously published individuals who harbor biallelic pathogenic variants in the *CAPN15* gene. Biallelic missense variants have been reported to demonstrate a phenotype of eye abnormalities and developmental delay, while biallelic loss of function variants exhibit phenotypes including microcephaly and craniofacial abnormalities, cardiac and genitourinary malformations, and abnormal neurologic activity. We report six individuals from three unrelated families harboring biallelic deleterious variants in *CAPN15* with phenotypes overlapping those previously described for this disorder. Of the individuals affected, four demonstrate radiographic evidence of the classical triad of Dandy-Walker malformation including hypoplastic vermis, fourth ventricle enlargement, and torcular elevation. Cerebellar anomalies have not been previously reported in association with *CAPN15*-related disease. Here, we present three unrelated families with findings consistent with oculogastrointestinal neurodevelopmental syndrome and cerebellar pathology including Dandy-Walker malformation. To corroborate these novel clinical findings, we present supporting data from the mouse model suggesting an important role for this protein in normal cerebellar development. Our findings add six molecularly confirmed cases to the literature and additionally establish a new association of Dandy-Walker malformation with biallelic *CAPN15* variants, thereby expanding the neurologic spectrum among patients affected by *CAPN15*-related disease.

**Keywords**

Dandy-walker malformation; calpain; cerebellar dysgenesis; phenotype expansion; oculogastrointestinal neurodevelopmental disorder; Purkinje cells

## 1 Introduction

Oculogastrointestinal neurodevelopmental syndrome (OMIM #619318) has been described in seven previously published individuals who harbor biallelic pathogenic variants in the *CAPN15* gene. Biallelic missense variants have been reported to demonstrate a phenotype of eye abnormalities and developmental delay, while biallelic loss of function variants exhibit phenotypes including microcephaly and craniofacial abnormalities, cardiac and genitourinary malformations, and abnormal neurologic activity.

Zha et al. first reported a series of five patients with eye malformations found to have biallelic missense variation in *CAPN15* (Zha et al., 2020). A subset of these patients additionally displayed developmental and cognitive delays, autism and congenital anomalies (summarized in Table 1). Mor-Shaked et al. reported two brothers with a homozygous C-terminal splice variant in *CAPN15*, found to have microcephaly, failure to thrive, developmental delay, seizures, abnormal brain morphology, and a similar spectrum of congenital anomalies (summarized in Table 1) (Mor-Shaked et al., 2021).

Little is known about the function of *CAPN15* despite its ubiquitous expression in the adult (GTEx Analysis Release V8 (Consortium, 2020), gtexportal.org). An atypical calpain, CAPN15 is composed of three domains: a 5’ region containing RanBP2-motif zinc fingers, a central calpain protease domain, and a 3’ domain with high homology to the drosophila *small optic lobes* (Sol) locus (Kamei et al., 1998). Other calpains are associated with both

neurodevelopmental and non-neurodevelopmental disease (Sorimachi et al., 2011; Velez et al., 2018). Though CAPN15 shares the catalytic calpain domain with the rest of the members of this class, its atypical N-terminal zinc fingers and unique C-terminal SOLH domain may confer distinctive functions.

Work in *Drosophila* has revealed roles for the *CAPN15* homolog, Sol, in the maintenance of neurons in the optic tracts; mutant ganglion cells degenerate during differentiation after failing to establish a significant number of functional contacts (Fischbach & Heisenberg, 1981). This degeneration leads to a significantly reduced brain volume. Similar findings are observed in the mouse: *Capn15* knockout mice have smaller brains with volume decreases in the thalamus and hippocampus (Zha et al., 2020).

Though cortical abnormalities have been described in both humans and animal models with *CAPN15* variation, no significant phenotypes have been noted in the hindbrain to date. Here, we present three independent families with biallelic *CAPN15* variation presenting with syndromic features characteristic of *CAPN15*-related disease in addition to the novel finding of cerebellar dysgenesis and Dandy-Walker malformation. This novel human genetic association suggests a role for *CAPN15* in hindbrain development.

## 2 Materials and Methods

### 2.1 Editorial Policies and Ethical Considerations

All participants in the study provided written informed consent in accordance with the institutional review boards at Duke University and University of California, San Diego. All participants provided consent for publication of deidentified clinical information and genome sequence data.

### 2.2 Rapid Whole Genome Sequencing (WGS)

Proband whole genome sequencing (WGS) was performed at Rady Children's Institute for Genomic Medicine as previously described (Kingsmore et al., 2019; Sanford et al., 2020). Sequencing libraries were prepared from whole blood-isolated DNA with the Illumina DNA PCR-Free Library Prep kit. A NovaSeq 6000 instrument and S1 flow cell (Illumina) were used to generate paired-end reads. DRAGEN Software Version 3.7.5 (Illumina) was used to call single nucleotide variants and insertions/deletions, as well as to align reads to reference assembly GRCh37/hg19. Structural variants/ copy number variants calling was performed based on coverage and soft clipped reads using DRAGEN-SV and DRAGEN-CNV algorithms (Illumina). Fabric Enterprise version 6.14.3 (Fabric Genomics) was used to annotate copy number variants and single nucleotide variants, and indels. The Genome Aggregation Database was used to filter those SNVs/indels with allelic balance between 0.3 and 0.7 and allele frequency <0.5%. Variants passing these filters were prioritized using Phevor Gene Rank (Kingsmore et al., 2019), and classified according to ACMG and AMP standards and guidelines (Richards et al., 2015). Only those CNVs occurring in areas with known or possible disease association were retained, and these were classified using ACMG and ClinGen guidelines (Riggs et al., 2020).

Human Phenotype Ontology (HPO) terms used for variant interpretation included: Dandy-Walker malformation (HP:0001305); Failure to thrive (HP:0001508); Small for gestational age (HP:0001518); Abnormality of the cardiovascular system (HP:0001626); Respiratory insufficiency (HP:0002093); Maternal diabetes (HP:0009800); Abnormal eye morphology (HP:0012372); Rectovestibular fistula (HP:0025025); Intraventricular hemorrhage (HP:0030746); Abnormality of coagulation (HP:0001928); Anal atresia (HP:0002023) and Macrocephaly (HP:0000256).

Variants of interest *PKP2* (NM_004572.4 c.235C>T, p.Arg79Ter) and *CAPN15* (NM_005632.3 c.2594T>C, p.Leu865Pro) were assessed by Custom Variant Analysis using Sanger Sequencing in the relatives of Family 3's proband after being reported in the proband.

### 2.3 Chromosomal Microarray

Chromosomal Microarray Analysis (CMA SNP) was performed using the Cytoscan HD array (Thermofisher). This array consists of nearly 2.7 million genetic markers incorporating 743,304 single nucleotide polymorphism (SNP) probes as well as 1,953,246 non polymorphic copy number variation (CNV) probes with a median spacing of 0.88 kb. In brief, genomic DNA was enzymatically digested, amplified, and purified. Purified products were fragmented, labeled, and hybridized to the array. Washed arrays (Affymetrix Fluidics Station 450), are scanned (Affymetrix GeneChip Scanner 3000) and analyzed using the Affymetrix ChAS software. Patient hybridization data were compared to a reference model. Copy number changes in regions of known benign copy number polymorphism were not reported. Deletions >300 kb, duplications >500 kb, and regions of homozygosity that exceed 10 Mb were evaluated and reported. Genomic linear positions were given relative to NCBI build 37 (hg19).

### 2.4 Whole Exome Sequencing

40x Illumina exome sequencing was performed using the IDT xGen™ Exome Research Panel v2. All variants were confirmed with Sanger sequencing and were tested for segregation in the entire family including unaffected members. All variants segregated in a manner demonstrating autosomal recessive inheritance.

### 2.5 In Silico Analyses

CAPN15 binary protein interaction data was generated from the Uniprot database (www.uniprot.org, O75808 CAN15_HUMAN). Binary protein interactions of all calpains (Supporting Information) were compared to this list to determine unique binding partners of CAPN15.

Protein structure information was derived from the AlphaFold prediction algorithm (AlphaFoldDB, www.alphafold.ebi.ac.uk, AF-O75808-F1). The highly structured region containing Family 3's variant, Leu865Pro, is predicted with very high confidence in the AlphaFold model. The effects of the Leu865Pro variant were modeled with SiteDirectedMutator (http://marid.bioc.cam.ac.uk/sdm2) by overlaying the familial variant over the AlphaFold predicted crystal structure of CAPN15.

Population-level variant and conservation analysis was conducted using the Genome Aggregation Database (gnomAD, https://gnomad.broadinstitute.org), Localized Intolerance Model using Bayesian Regression model (LIMBR, https:/tris-10.github.io/limbr/index.html), and Multiz Alignments of 30 Vertebrates (accessed through UCSC Genome Browser, https://genome.ucsc.edu), PhastCons (accessed through the UCSC Genome Browser, https://genome.ucsc.edu), and PhyloP (evaluated through CADD algorithm, http://cadd.gs.washington.edu).

Variant pathogenicity determination was computed with the Combined Annotation Dependent Depletion algorithm (CADD, http://cadd.gs.washington.edu). This score incorporates projections from SIFT (http://sift.bii.a-star.edu.sg) and PolyPhen2 (http://genetics.bwh.harvard.edu), which predict amino acid substitution effect on protein function. REVEL (https://sites.google.com/site/revelgenomics/) was also used to corroborate missense variant effect predictions (accessed through the UCSC Genome Browser, http://genome.ucsc.edu).

Reference data for tissue-specific gene expression was derived from the Genotype-Tissue Expression Portal v8 release (GTEx, https://gtexportal.org).

### 2.6 Western Blot

Whole cell fibroblast lysates were boiled directly in sample buffer and run on a 10% SDS-PAGE gel, probed with antibodies for SOLH (ABCAM 1:1000, Anti-Calpain 15/SOLH antibody (cat# ab241074)) and GAPDH (ABCAM Anti-GAPDH antibody - Loading Control (ab9485) 1:2000) and visualized by chemiluminescence (Pierce).

### 2.7 RT-PCR

A reaction to target CAPN15 with forward primer CTGACCTCATCTGGGCCAAA and reverse primer CGTGCGGCATGAGCTGCCA was run on cDNA generated from patient fibroblast RNA using Qiagen PCR reagents, producing a product of 276bp. GAPDH control was amplified with forward primer GTGGAGTCCACTGGCGTCTTC and reverse primer CTCGACGCCTGCTTCACCAC. Thirty-five PCR cycles were run at 60 degree melting temperatures. A negative control lane utilized water in place of DNA.

### 2.8 Immunofluorescence

Mice were sacrificed and perfusion fixed with 4% PFA in PBS, then cryoprotected with 30% sucrose and mounted in OCT. 20μm sections of the cerebellar hemisphere lateral to the vermis from approximately the IV/V lobule were blocked with 4% donkey serum, and stained with primary antibodies (ABCAM 1:1000, Anti-Calpain 15/SOLH antibody cat# ab241074; calbindin-D-28K antibody produced in mouse, Sigma c9848) overnight. Incubation with secondary antibodies (Jackson ImmunoResearch AffiniPure goat anti-rabbit FITC conjugated IgG cat# 111–095-003; AffiniPure goat anti-mouse Alexa 594 conjugated IgG cat# 115–585-003) occurred prior to visualization on a Leica SP8 confocal microscope.

# 3 Results

## 3.1 Part One: Case presentations

We report six individuals from three unrelated families harboring biallelic variants in *CAPN15* with phenotypes overlapping those previously described for this disorder. Of these individuals affected, four of five with neuroimaging available demonstrate radiographic evidence of the classical triad of Dandy-Walker malformation including hypoplastic vermis, fourth ventricle enlargement, and torcular elevation. Families 1 and 2 have received molecular diagnoses since their phenotypes were initially described in detail in a previously published case series by coauthors Zaki, Masri, Gregor, and Gleeson (Zaki et al., 2015).

**3.1.1 Family 1—**Family 1 was described in detail previously by Zaki et al. (DWM- 927) (Zaki et al., 2015). In brief, the proband was born to first-cousin consanguineous parents and presented with several dysmorphic features including broad forehead, sparse eyebrows, and underdeveloped ala nasi. She had persistent microcephaly and poor weight gain along with global developmental delay and hypotonia. She presented with several congenital anomalies including anal atresia with a single cloacal opening, underdeveloped labia majora, small kidneys, broad halluces, and bilateral single transverse palmar crease. MRI revealed significant hypoplastic vermis and findings consistent with Dandy-Walker malformation. A similarly affected, deceased first cousin of the proband, also a product of a first-cousin consanguineous union, was reported to have intellectual disability, microcephaly, failure to thrive, hypotonia, arthrogryposis, and unilateral preaxial polydactyly. Chromosomal microarray was non-diagnostic and subsequent research exome sequencing of the proband and parents revealed homozygosity in the proband for a pathogenic variant in *CAPN15* (NM_005632.3 c.2164delC, p.Arg716Glyfs*99); this frameshift variant in exon 8 results in a premature truncation of the transcript (Figure 1).

**3.1.2 Family 2—**Clinical findings were described in detail in a previous publication (DWM-1040) (Zaki et al., 2015). Briefly, the proband and an affected first cousin were both born to consanguineous unions. The proband presented with several dysmorphic features including broad forehead, underdeveloped ala nasi, and overhanging nasal tip. She had a single kidney and an imperforate anus. She exhibited hypotonia and sensorineural deafness. MRI showed a hypoplastic vermis and mega cisterna magna and was suggestive of Dandy-Walker malformation. The proband's affected cousin presented with similar dysmorphic features and microcephaly. This individual had hypoplastic kidneys, imperforate anus, and a urogenital fistula. She exhibited hypotonia, global developmental delay, sensorineural deafness, and had no development of speech. MRI showed mild ventriculomegaly and findings consistent with Dandy-Walker malformation. Chromosomal microarray was non-diagnostic and subsequent research exome and genome sequencing of both proband and cousin revealed homozygosity for a pathogenic frameshift variant in exon 4 of *CAPN15* (NM_005632.3 c.754dupC, p.Gln254Profs*7) that results in premature truncation of the transcript (Figure 1).

**3.1.3 Family 3—**Proband and an affected older sister were born to non-consanguineous parents. Proband exhibited dysmorphic features including anteverted nares and flattened

nasal bridge. Ocular findings included iridocorneal adhesions and bilateral corneal clouding. Proband was born with significant cardiac abnormalities including a stretched patent foramen ovale, large conoventricular septal defect, aortic valve atresia with severely hypoplastic aorta, and aberrant right subclavian artery. She had anal atresia with a rectovestibular fistula and a slightly asymmetric sacrum was noted on radiograph. She had ventriculomegaly and brain imaging findings suggestive of Dandy-Walker malformation including residual vermis and a large posterior fossa cyst (Figure 2B). No intra-abdominal abnormalities were visualized via ultrasound. The proband was critically ill in the neonatal period, suffering from intraventricular hemorrhage, thrombosis, and intraoperative circulatory failure requiring ECMO. On day of life 10 the patient died secondary to complications from her cardiac reconstructive surgery. The proband's older affected sister exhibited several eye findings including microphthalmos, strabismic amblyopia, monocular exotropia, and bilateral coloboma. She had pulmonic stenosis and persistent bilateral superior vena cavae, as well as bilateral small kidneys. Sacral anomalies included a sacral dimple and tethered spinal cord. Skeletal findings included bowing of legs, tight achilles, fifth finger clinodactyly, and overlapping toes. Her MRI findings were significant for severely enlarged ventricles and imaging findings consistent with Dandy-Walker malformation (Figure 2B). Family history was notable for mild intellectual disability, seizure disorder, and congenital heart disease in the proband and sibling's mother. Both the proband and her sister were found to carry biallelic variants affecting *CAPN15:* a whole-gene deletion as part of a maternally inherited chromosome 16p13.3 deletion: arr[hg19]16p13.3(84116_692192)x1 (Supporting Information) and a paternally inherited missense likely pathogenic variant (NM_005632.3 c.2594T>C, p.Leu865Pro) as shown in Figure 2A. In addition, the proband was also found to have a 439kb interstitial loss (deletion) at chromosome 15q11.2: arr[hg19]15q11.2(22770421_23209531)x1. This deletion was not thought to be contributing to her severe congenital anomalies.

### 3.2 Part two: Functional Validation of Variants

Families 1 and 2 were found to have homozygous frameshift variants resulting in premature termination of the *CAPN15* transcript. The frameshift variant in Family 1 results in a stop codon in the last exon of the transcript, which is not surveilled by nonsense-mediated decay machinery and thus does not result in degradation of mRNA. The frameshift variant in Family 2 results in a truncation much further upstream, leading to degradation of transcript via nonsense-mediated decay. Consistent with this, RT-PCR of the variant transcript showed a reduced intensity (Figure 3A, white arrows) in affected homozygotes compared to unaffected heterozygous relatives in Family 2, but not in Family 1 (Figure 3A). Western blot detection of the CAPN15 C-terminus however, demonstrates a total loss of this domain in affected, but not in unaffected, individuals of both families (Figure 3B).

Family 3 harbors a novel missense variant at residue 865 of the CAPN15 protein. This locus is highly conserved in vertebrate species (Figure 4A). The predicted CAPN15 three-dimensional structure generated by AlphaFold (Jumper et al., 2021) places LEU865 at the center of the protein, in a highly organized region at the interface of a beta sheet and alpha helix (Figure 4B). Using this predicted structure as the wild-type comparison, the presence of the variant amino acid p.Leu865Pro is predicted by Site Directed Mutator

(Pandurangan et al., 2017) to significantly decrease protein stability (ΔΔG = −3.98). In silico tools SIFT (Ng & Henikoff, 2003), Polyphen2 (Adzhubei et al., 2010), and REVEL (Ioannidis et al., 2016) are consistent in their prediction of this missense variant being deleterious: scores SIFT 0 deleterious, PolyPhen 0.98 probably_damaging, REVEL 0.848. Furthermore, this variant is not found in any healthy individuals in the gnomAD database (Gudmundsson et al., 2021); the Limbr (Hayeck et al., 2019), PhyloP (Pollard et al., 2010), and PhastCons (Siepel et al., 2005) algorithms predict that this variant's locus is strongly constrained against missense variation (Figure 4C): scores Limbr 0.206 percentile, PhyloP vertebrate 6.665, PhastCons vertebrate 1. Lastly, CADD (Rentzsch et al., 2019), an integrated deleteriousness prediction algorithm, categorizes p.Leu865Pro as one of the 1% most deleterious possible mutations in the genome: raw score 3.645, PHRED 25.2. While the affected childrens' father, who is heterozygous for this variant, is asymptomatic, the combination of this variant with a maternally inherited deletion appears to unmask its deleterious nature in both affected children.

### 3.3 Part Three: CAPN15 loss of function is associated with a spectrum of neurodevelopmental abnormalities spanning from mild intellectual disability to cerebellar dysgenesis

Because nearly all patients with *CAPN15* biallelic variation have intellectual disability or delay of developmental milestones (Table 1; 10/10 who underwent neurodevelopmental evaluation), we sought to better understand the role of *CAPN15* in neurodevelopment. Interestingly, patients with biallelic missense variants in *CAPN15* are only reported to have mild neurodevelopmental phenotypes, manifesting as speech or motor delay, intellectual disability, or autism spectrum disorder (Zha et al., 2020). Individuals with an intronic deletion resulting in exon skipping and frameshift of the C-terminus of the protein have slightly more involved neurological phenotypes, including seizure, cortical thinning, and ventriculomegaly (Mor-Shaked et al., 2021). Patients with *CAPN15* loss of function variants are reported to demonstrate cerebellar dysgenesis and Dandy Walker malformation. Since not all individuals with *CAPN15* variants have had brain imaging, and furthermore, since Dandy-Walker malformation may be overlooked even when imaging is conducted, it is difficult to determine a genotype-phenotype correlation at this time.

### 3.4 Part Four: CAPN15 expression in mouse cerebellum

In the mouse, cerebellar progenitors are formed between E12.5 and E14.5 and continue to mature through the postnatal period (Mizuhara et al., 2010). It has previously been shown that *Capn15* is enriched in the Purkinje cells of the mature cerebellum (Zha et al., 2021), though expression patterns earlier in the developmental course are unknown. We replicate this finding, and also show expression of CAPN15/SOLH in maturing Purkinje cells in early postnatal development (Figure 5), suggesting that the protein plays a role in both the developing and mature cerebellum.

Staining of the developing mouse cerebellar hemisphere at postnatal days 5 and 11 demonstrates expression of CAPN15/SOLH in Purkinje cells, as indicated by coexpression with calbindin. Additional faint non-nuclear staining can be seen superior to the Purkinje

cells, in the molecular layer, as well as inferior to the Purkinje cells in the granular zone layer.

Since molecular characterization of CAPN15 is limited, we turned to pre-existing datasets and computational characterization to understand what unique roles CAPN15 may be playing in the cerebellum to contribute to dysgenesis and Dandy-Walker malformation. We searched for CAPN15 binary binding interactions predicted by UniProt (https://www.uniprot.org) (UniProt, 2021). Interestingly, of the 6 binding partners identified via this method (Table 2), none were shared by any other members of the calpain class (Supporting Information). CAPN15 binding partners have roles in the ubiquitin/proteasome pathways and in the promotion of cell division. These roles are consistent with observed properties of CAPN15 in polyubiquitin binding (Hastings et al., 2018) and cell survival (Fischbach & Heisenberg, 1981; Fischbach & Technau, 1984; Zha et al., 2021) observed in animal models.

## 4 Discussion

Cerebellar anomalies have not been previously reported in association with *CAPN15*-related disease. Here we present six individuals from three unrelated families who display findings consistent with oculogastrointestinal neurodevelopmental syndrome in addition to cerebellar pathology including Dandy-Walker malformation. To corroborate these novel clinical findings, we present supporting evidence of prominent CAPN15 protein expression in Purkinje cells in the postnatal and adult mouse that suggest an important role for CAPN15 in normal cerebellar development. Our findings add six molecularly confirmed patient cases to the literature and additionally establish a new association of Dandy-Walker malformation with biallelic *CAPN15* variants, thereby expanding the neurologic phenotype associated with this condition.

Though our analysis is restricted to postnatal maturation of the cerebellum, and is later than the earliest known presentations of Dandy-Walker malformation (Haldipur et al., 2021), a role for CAPN15 in prenatal cerebellar development may still be possible. Analysis of fetal cerebellar single-cell RNA sequencing (Aldinger et al., 2021) revealed low-level expression of *CAPN15* in numerous cell populations, including Purkinje cells, the rhombic lip, granule cell progenitors, and granule neurons as early as 9 weeks postconception. Though prior work has shown aberrancies in the development of the rhombic lip, a site of glutamatergic neuron proliferation, in the etiology of Dandy-Walker malformation (Haldipur et al., 2021), *CAPN15* was not found to be significantly differentially expressed between patients with Dandy-Walker malformation and healthy controls in this cell population. Indeed, further investigations in both the mouse and human will be critical to fully understand the role of CAPN15 expression in the development of the cerebellum, and to link this gene to those pathways already known to play a role in Dandy-Walker malformation.

We report a novel likely pathogenic missense variant in Family 3 contained in the SOLH domain of the CAPN15 protein. This variant is predicted to significantly destabilize the protein ($\Delta\Delta G = -3.98$ p.Leu865Pro), which is consistent with two other known homozygous pathogenic variants also reported to destabilize the SOLH domain ($\Delta\Delta G = -3.27$ p.Gly969Ser; $\Delta\Delta G = -1.15$ p.Arg1028Lys) (Pandurangan et al., 2017; Zha et al.,

2020) at highly conserved residues. In Family 3, the p.Leu865Pro variant is *in trans* with a whole gene deletion, unmasking a dosage-dependent and stability-dependent deleterious phenotype, seemingly more severe than those with isolated SOLH domain-destabilizing point mutations.

By comparing the patients with biallelic *CAPN15* loss of function variants and Dandy-Walker malformation to those previously reported individuals with *CAPN15* variants, it is possible that neurological severity may correlate with the severity of variant effect on the *CAPN15* transcript and protein. This spectrum of phenotype may suggest that the dosage of functional CAPN15 is critical for proper neurodevelopment, and that a threshold amount of functional protein is necessary for formation of the cerebellum. Genotype-phenotype correlation is an area that requires further investigation for *CAPN15,* however, as Dandy-Walker malformation may have been overlooked in previously diagnosed patients. The new knowledge of Dandy-Walker malformation as a phenotype that may present in individuals with *CAPN15*-related disease, may allow for systematic investigation of this feature on brain imaging among future individuals diagnosed. Interestingly, the mother in Family 3, who carries a 16p13.3 deletion resulting in a heterozygous deletion of *CAPN15* (and 30 other genes, Supporting Information), lacks several of the congenital anomalies characteristic of oculogastrointestinal neurodevelopmental syndrome but does report intellectual disability and anemia. Further examination of the maternal family history revealed several family members with intellectual disability, ADHD, and autism spectrum-like features, as well as anemia consistent with ATR-16 syndrome (MIM #141750) known to be associated with deletions in this region (Supporting Information).

Our assessment of the cerebellar mechanisms of CAPN15 is limited by a focus on the cortical and optic tract phenotypes in animal models of *CAPN15*-related disease. The *Capn*15$^{-/-}$ mouse has many features of oculogastrointestinal neurodevelopmental syndrome but does not have explicit cerebellar dysgenesis (Zha et al., 2020). However, by volumetric MRI evaluation, Zha *et al* noted a decrease in volume of the cerebellum in knockout mice (Zha et al., 2021). PCP4+ cell counting in adult knockout mice did not reveal a statistically significant decrease of Purkinje cells. The authors noted that only viable mice were evaluated; it is possible that mice with severely affected cerebella do not survive to adulthood. While it may be that the lack of Dandy-Walker malformation in *Capn15*$^{-/-}$ mice is attributable to inherent differences between mouse and human development or statistical underpowering of the analysis, further evaluation of embryonic, juvenile, and prematurely lethal *Capn15*$^{-/-}$ mice is necessary to fully establish the extent of the cerebellar phenotype in this model. Though the CAPN15 antibody used in this report has not been published previously, our findings of CAPN15/SOLH in Purkinje cells are consistent with those reported in the Zha et al. mouse studies. Further investigation will be required to characterize the full spatiotemporal landscape of CAPN15 expression in the mouse cerebellum as well as the effect of human variants on CAPN15 function in Purkinje cells.

Further mechanistic work is required to fully elucidate the mechanism of *CAPN15* in cerebellar development. Our findings demonstrate a novel disease association of *CAPN15* loss of function with Dandy-Walker malformation, or agenesis of the cerebellum. This novel disease association and implication of CAPN15 function in new regions of the brain opens

up pathways to explore interactions between the known cortical roles of synaptic plasticity, cytoskeleton remodeling, and cell proliferation in the proper maturation of the cerebellum.

## Supplementary Material

Refer to Web version on PubMed Central for supplementary material.

## Acknowledgements

Thank you to the patients and families for their participation in this research. The authors thank Gregory Crawford and Anne West for critical review of results and helpful discussion of the manuscript. The authors thank Jeffrey Petrella for review of radiologic images.

### Funding Statement

Personnel effort for this work was provided by Duke University Medical Scientist Training Program T32GM007171-47 to M. Makenzie Beaman, Y.T and Alice Chen Pediatric Genetics and Genomics Research Center funding to Jennifer L. Cohen. Exome sequencing of Families 1 and 2, as well as mouse work was funded by NIH grant R01NS098004 to Joseph G. Gleeson. Genome sequencing analysis of Family 3 was funded by the Rady Children's Institute for Genomic Medicine. The WCG IRB costs and regulatory personnel effort were funded by the Neonatal Perinatal Research Unit at Duke University.

## Data Availability Statement

Variants described in this publication will be deposited in ClinVar [https://ncbi.nlm.nih.gov/clinvar/]. Additional data that support the findings of this study are available from the corresponding author upon reasonable request.

## References

Adzhubei IA, Schmidt S, Peshkin L, Ramensky VE, Gerasimova A, Bork P, Kondrashov AS, & Sunyaev SR (2010). A method and server for predicting damaging missense mutations. Nat Methods, 7(4), 248–249. 10.1038/nmeth0410-248 [PubMed: 20354512]

Aldinger KA, Thomson Z, Phelps IG, Haldipur P, Deng M, Timms AE, Hirano M, Santpere G, Roco C, Rosenberg AB, Lorente-Galdos B, Gulden FO, O'Day D, Overman LM, Lisgo SN, Alexandre P, Sestan N, Doherty D, Dobyns WB, . . . Millen KJ. (2021). Spatial and cell type transcriptional landscape of human cerebellar development. Nat Neurosci, 24, 1163–1175. [PubMed: 34140698]

Consortium, T. G. (2020). The GTEx Consortium atlas of genetic regulatory effects across human tissues. Science, 369, 1318–1330. [PubMed: 32913098]

Fischbach KF, & Heisenberg M (1981). Structural brain mutant of Drosophila melanogaster with reduced cell number in the medulla cortex and with normal optomotor yaw response. Proceedings of the National Academy of Sciences, 78(2), 1105–1108.

Fischbach KF, & Technau G (1984). Cell Degeneration in the Developing Optic Lobes of the sine oculis and small-optic-lobes Mutants of Drosophila melanogaster. Dev biool, 194, 219–239.

Gudmundsson S, Singer-Berk M, Watts NA, Phu W, Goodrich JK, Solomonson M, Genome Aggregation Database C, Rehm HL, MacArthur DG, & O'Donnell-Luria A (2021). Variant interpretation using population databases: Lessons from gnomAD. Hum Mutat. 10.1002/humu.24309

Haldipur P, Bernardo S, Aldinger KA, Sivakumar T, Millman J, Sjoboen AH, Dang D, Dubocanin D, Deng M, Timms AE, Davis BD, Plummer JT, Mankad K, Oztekin O, Manganaro L, Guimiot F, Adle-Biassette H, Russo R, Siebert JR, . . . Millen KJ. (2021). Evidence of disrupted rhombic lip development in the pathogenesis of Dandy-Walker malformation. Acta Neuropathologica, 142, 761–776. 10.1007/s00401-021-02355-7 [PubMed: 34347142]

Hastings MH, Qiu A, Zha C, Farah CA, Mahdid Y, Ferguson L, & Sossin WS (2018). The zinc fingers of the small optic lobes calpain bind polyubiquitin. J Neurochem, 146(4), 429–445. 10.1111/jnc.14473 [PubMed: 29808476]

Hayeck TJ, Stong N, Wolock CJ, Copeland B, Kamalakaran S, Goldstein DB, & Allen AS (2019). Improved Pathogenic Variant Localization via a Hierarchical Model of Sub-regional Intolerance. Am J Hum Genet, 104(2), 299–309. 10.1016/j.ajhg.2018.12.020 [PubMed: 30686509]

Ioannidis NM, Rothstein JH, Pejaver V, Middha S, McDonnell SK, Baheti S, Musolf A, Li Q, Holzinger E, Karyadi D, Cannon-Albright LA, Teerlink CC, Stanford JL, Isaacs WB, Xu J, Cooney KA, Lange EM, Schleutker J, Carpten JD, . . . Sieh W. (2016). REVEL: An Ensemble Method for Predicting the Pathogenicity of Rare Missense Variants. Am J Hum Genet, 99(4), 877–885. 10.1016/j.ajhg.2016.08.016 [PubMed: 27666373]

Jumper J, Evans R, Pritzel A, Green T, Figurnov M, Ronneberger O, Tunyasuvunakool K, Bates R, Zidek A, Potapenko A, Bridgland A, Meyer C, Kohl SAA, Ballard AJ, Cowie A, Romera-Paredes B, Nikolov S, Jain R, Adler J, . . . Hassabis D. (2021). Highly accurate protein structure prediction with AlphaFold. Nature, 596(7873), 583–589. 10.1038/s41586-021-03819-2 [PubMed: 34265844]

Kamei M, Webb GC, Young IG, & Campbell HD (1998). SOLH, a Human Homologue of the Drosophila melanogaster small optic lobes Gene Is A Member of the Calpain and Zinc-Finger Gene Families and Maps to Human Chromosome 16p13.3 near CATM (Cataract with Microphthalmia). Genomics, 51, 197–206, Article GE985395. [PubMed: 9722942]

Kingsmore SF, Cakici JA, Clark MM, Gaughran M, Feddock M, Batalov S, Bainbridge MN, Carroll J, Caylor SA, Clarke C, Ding Y, Ellsworth K, Farnaes L, Hildreth A, Hobbs C, James K, Kint CI, Lenberg J, Nahas S, . . . Investigators, R. (2019). A Randomized, Controlled Trial of the Analytic and Diagnostic Performance of Singleton and Trio, Rapid Genome and Exome Sequencing in Ill Infants. Am J Hum Genet, 105(4), 719–733. 10.1016/j.ajhg.2019.08.009 [PubMed: 31564432]

Mizuhara E, Minaki Y, Nakatani T, Kumai M, Inoue T, Muguruma K, Sasai Y, & Ono Y (2010). Purkinje cells originate from cerebellar ventricular zone progenitors positive for Neph3 and E-cadherin. Dev Biol, 338(2), 202–214. 10.1016/j.ydbio.2009.11.032 [PubMed: 20004188]

Mor-Shaked H, Salah S, Yanovsky-Dagan S, Meiner V, Atawneh OM, Abu-Libdeh B, Elpeleg O, & Harel T (2021). Biallelic deletion in a minimal CAPN15 intron in siblings with a recognizable syndrome of congenital malformations and developmental delay. Clin Genet, 99(4), 577–582. 10.1111/cge.13920 [PubMed: 33410501]

Ng PC, & Henikoff S (2003). SIFT: Predicting amino acid changes that affect protein function. Nucleic Acids Res, 31(13), 3812–3814. 10.1093/nar/gkg509 [PubMed: 12824425]

Pandurangan AP, Ochoa-Montano B, Ascher DB, & Blundell TL (2017). SDM: a server for predicting effects of mutations on protein stability. Nucleic Acids Res, 45(W1), W229–W235. 10.1093/nar/gkx439 [PubMed: 28525590]

Pollard KS, Hubisz MJ, Rosenbloom KR, & Siepel A (2010). Detection of nonneutral substitution rates on mammalian phylogenies. Genome Res, 20(1), 110–121. 10.1101/gr.097857.109 [PubMed: 19858363]

Rentzsch P, Witten D, Cooper GM, Shendure J, & Kircher M (2019). CADD: predicting the deleteriousness of variants throughout the human genome. Nucleic Acids Res, 47(D1), D886–D894. 10.1093/nar/gky1016 [PubMed: 30371827]

Richards S, Aziz N, Bale S, Bick D, Das S, Gastier-Foster J, Grody WW, Hegde M, Lyon E, Spector E, Voelkerding K, Rehm HL, & Committee ALQA (2015). Standards and guidelines for the interpretation of sequence variants: a joint consensus recommendation of the American College of Medical Genetics and Genomics and the Association for Molecular Pathology. Genet Med, 17(5), 405–424. 10.1038/gim.2015.30 [PubMed: 25741868]

Riggs ER, Andersen EF, Cherry AM, Kantarci S, Kearney H, Patel A, Raca G, Ritter DI, South ST, Thorland EC, Pineda-Alvarez D, Aradhya S, & Martin CL (2020). Technical standards for the interpretation and reporting of constitutional copy-number variants: a joint consensus recommendation of the American College of Medical Genetics and Genomics (ACMG) and the Clinical Genome Resource (ClinGen). Genet Med, 22(2), 245–257. 10.1038/s41436-019-0686-8 [PubMed: 31690835]

Sanford E, Wong T, Ellsworth KA, Ingulli E, & Kingsmore SF (2020). Clinical utility of ultra-rapid whole-genome sequencing in an infant with atypical presentation of WT1-associated nephrotic

syndrome type 4. Cold Spring Harb Mol Case Stud, 6, a005470. 10.1101/mcs.a005470 [PubMed: 32843431]

Siepel A, Bejerano G, Pedersen JS, Hinrichs AS, Hou M, Rosenbloom K, Clawson H, Spieth J, Hillier LW, Richards S, Weinstock GM, Wilson RK, Gibbs RA, Kent WJ, Miller W, & Haussler D (2005). Evolutionarily conserved elements in vertebrate, insect, worm, and yeast genomes. Genome Res, 15(8), 1034–1050. 10.1101/gr.3715005 [PubMed: 16024819]

Sorimachi H, Hata S, & Ono Y (2011). Calpain chronicle--an enzyme family under multidisciplinary characterization. Proc Jpn Acad Ser B Phys Biol Sci, 87(6), 287–327. 10.2183/pjab.87.287

UniProt C (2021). UniProt: the universal protein knowledgebase in 2021. Nucleic Acids Res, 49(D1), D480–D489. 10.1093/nar/gkaa1100 [PubMed: 33237286]

Velez G, Bassuk AG, Schaefer KA, Brooks B, Gakhar L, Mahajan M, Kahn P, Tsang SH, Ferguson PJ, & Mahajan VB (2018). A novel de novo CAPN5 mutation in a patient with inflammatory vitreoretinopathy, hearing loss, and developmental delay. Cold Spring Harb Mol Case Stud, 4(3). 10.1101/mcs.a002519

Zaki MS, Masri A, Gregor A, Gleeson JG, & Rosti RO (2015). Dandy-Walker malformation, genitourinary abnormalities, and intellectual disability in two families. Am J Med Genet A, 167A(11), 2503–2507. 10.1002/ajmg.a.37225 [PubMed: 26109232]

Zha C, Farah CA, Fonov V, Rudko DA, & Sossin WS (2021). MRI of Capn15 Knockout Mice and Analysis of Capn 15 Distribution Reveal Possible Roles in Brain Development and Plasticity. Neuroscience, 465, 128–141. 10.1016/j.neuroscience.2021.04.023 [PubMed: 33951504]

Zha C, Farah CA, Holt RJ, Ceroni F, Al-Abdi L, Thuriot F, Khan AO, Helaby R, Levesque S, Alkuraya FS, Kraus A, Ragge NK, & Sossin WS (2020). Biallelic variants in the small optic lobe calpain CAPN15 are associated with congenital eye anomalies, deafness and other neurodevelopmental deficits. Hum Mol Genet, 29(18), 3054–3063. 10.1093/hmg/ddaa198 [PubMed: 32885237]

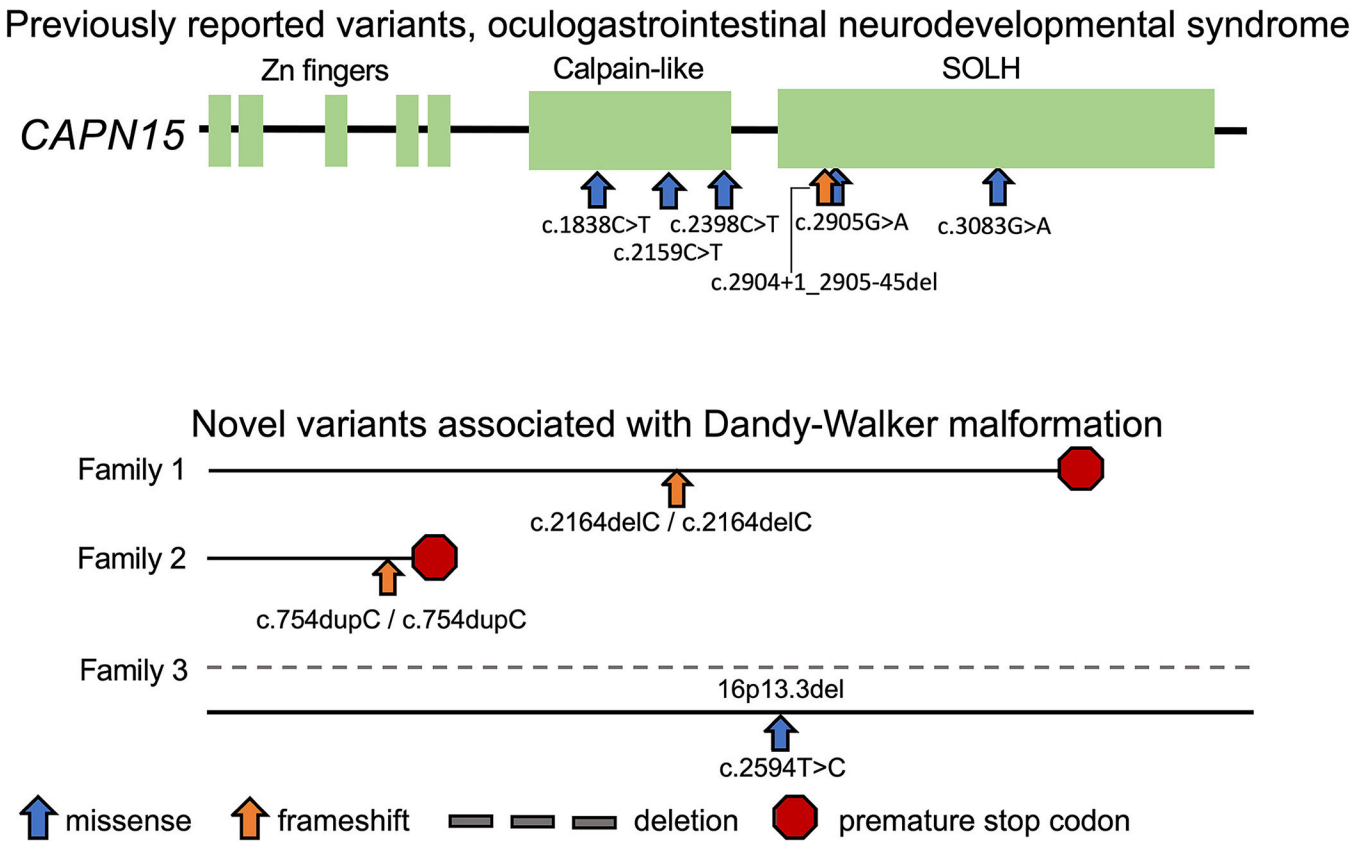


**Figure 1. Molecular consequence of *CAPN15* variation and reported phenotype presentations.**

Previously reported patients with mild neurodevelopmental phenotypes have predominantly missense variants in *CAPN15*, while novel frameshift variants and full gene deletions present with Dandy-Walker malformation. A previously reported frameshift variant c.2904+1_2905–45del (Mor-Shaked et al., 2021) leads to skipping of an exon and was reported with more severe brain involvement including cortical thinning. Cerebellar phenotypes were not specified in the siblings with this variant.

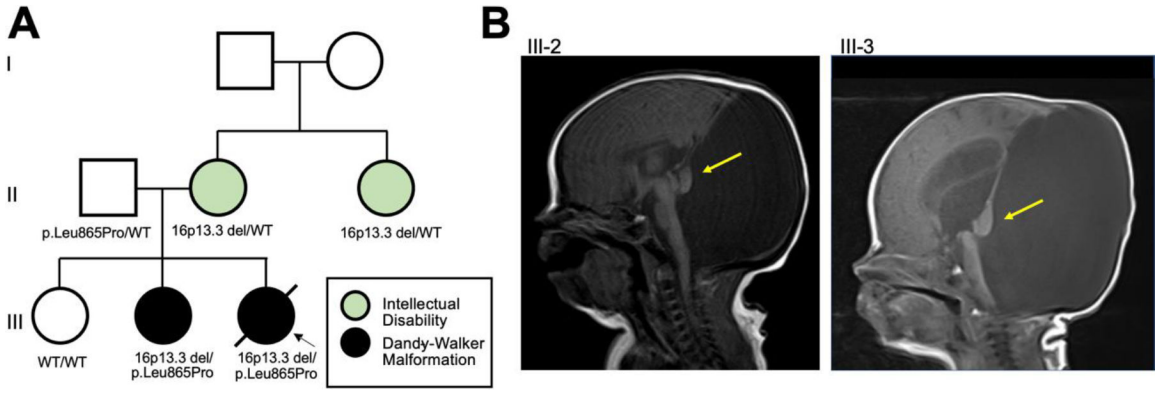


**Figure 2. Dandy-Walker malformation segregates with biallelic deleterious variants in *CAPN15*.**

A) Pedigree for Family 1 demonstrating two affected siblings. Proband (III-3) and affected sister (III-2) both inherited biallelic *CAPN15* variants and presented with Dandy-Walker malformation. Heterozygous carriers of the p.Leu865Pro variant do not present with typical syndromic features of oculogastrointestinal neurodevelopmental syndrome. Individuals II-2 and II-3, who are heterozygous for 16p13.3 deletion, present with intellectual disability, which is consistent with the ATR-16 phenotype (MIM #141750) associated with heterozygous deletion of this region. Unaffected sibling III-1 demonstrated absence of both the 16p13.3 deletion and the *CAPN15* familial variant. B) Brain imaging for Family 1 demonstrating confirmed Dandy-Walker Malformation in both siblings. III-2 and III-3 show residual vermis (yellow arrows). Additional findings for both images: lambdoidal torcular elevation and large posterior fossa cysts splaying the cerebellar hemispheres. III-2 shows mild hydrocephalus; III-3 shows severe hydrocephalus.

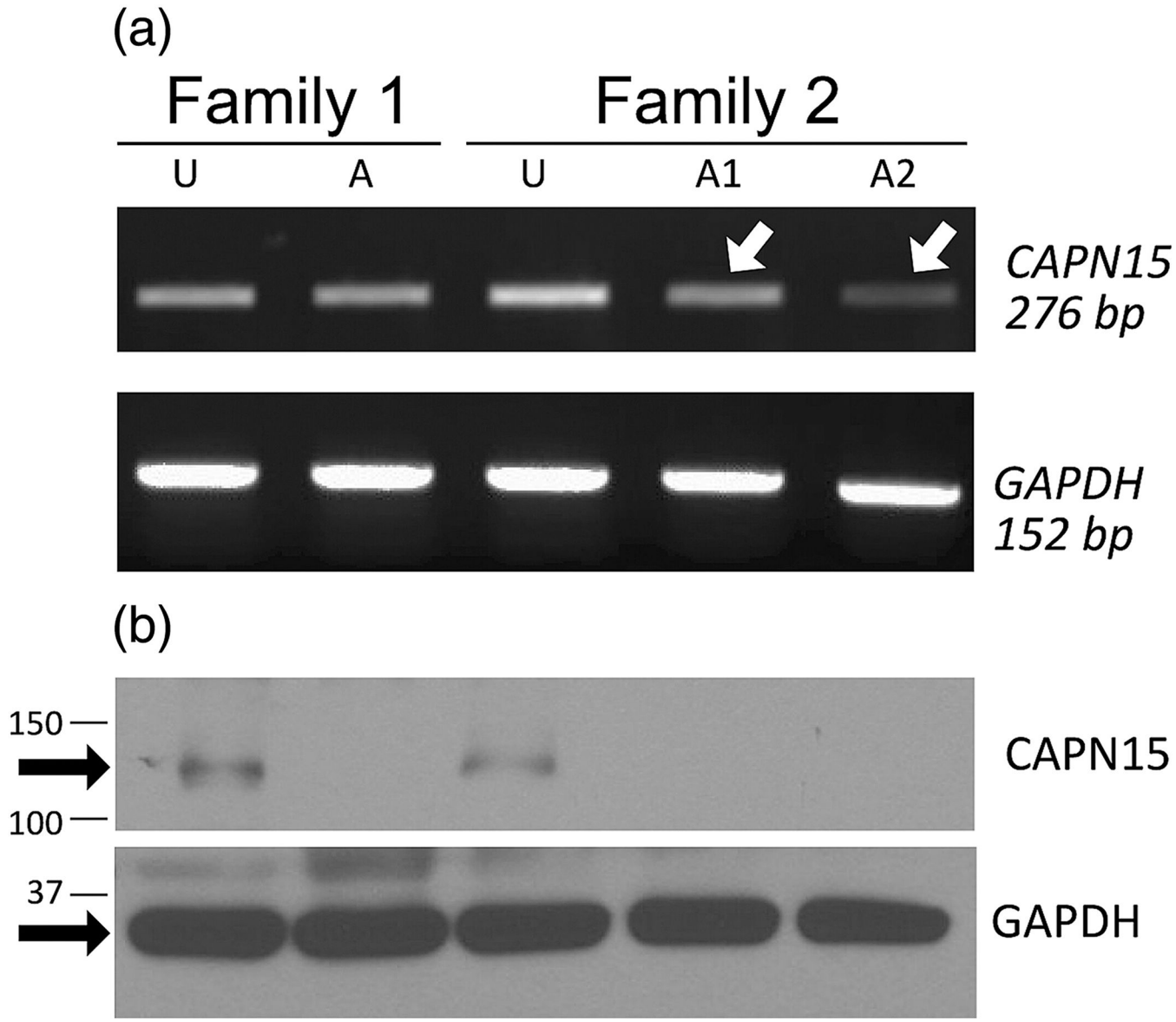


**Figure 3. Frameshift variants found in Families 1 and 2 result in a loss of CAPN15 C-terminus.**

RT-PCR (a) and Western Blot (b) of probands (A, A1, A2) and unaffected (U) heterozygous parents in Family 1 (p.Arg716Glyfs*99) and Family 2 (p.Gln254Profs*7). Reduced mRNA expression is found in affected homozygotes of Family 2, but not Family 1 compared to unaffected heterozygous parents. In both cases, there is a loss of full-length protein expression as indicated by a lack of staining by an antibody directed at the C-terminus of CAPN15.

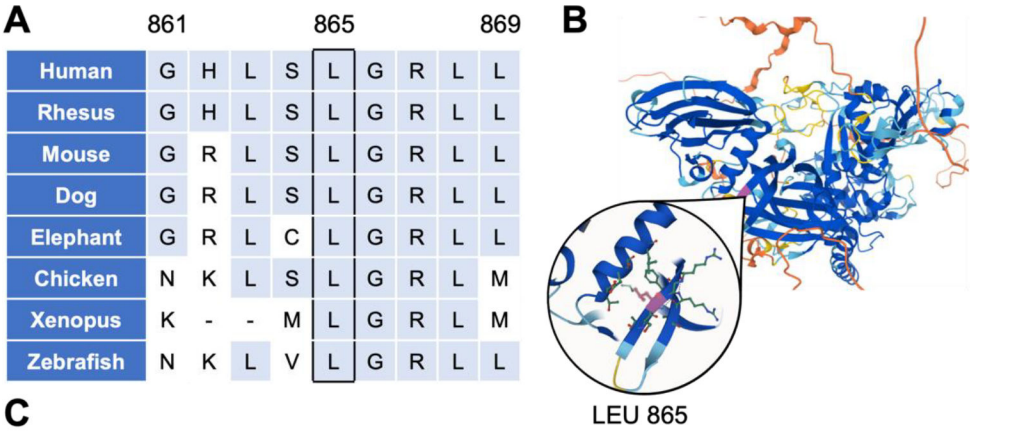


| Resource | Reference | Evaluation | Score | Prediction |
|---|---|---|---|---|
| GnomAD v2.1.1 | Karczewski, *Nature* (2020) | Population variation | 0 individuals | p.Leu865Pro not found in healthy individuals |
| Limbr | Hayeck, *AJHG* (2019) | Sequence constraint | raw score -46.962 0.206 percentile | LEU865 strongly constrained against missense variation |
| CADD v1.6 | Kircher, *Nat Genet* (2014) | Relative pathogenicity | raw score 3.645 PHRED 25.2 | p.Leu865Pro 1% most deleterious possible mutations in genome |

**Figure 4. Several *in silico* analyses support the pathogenicity of the novel p.Leu865Pro missense variant.**

(A) Leu865 is widely conserved across vertebrate species. *Sequences obtained via 100 Vertebrates MultiZ alignment.* (B) Alpha-fold predicted structure AF-O75080-F1 places Leu865 in a highly organized region central to the protein, interfacing between an alpha-helix and beta-sheet complex. (C) Several algorithms predict the variant to be deleterious, including measures of natural population variation, sequence constraint, and missense relative pathogenicity.

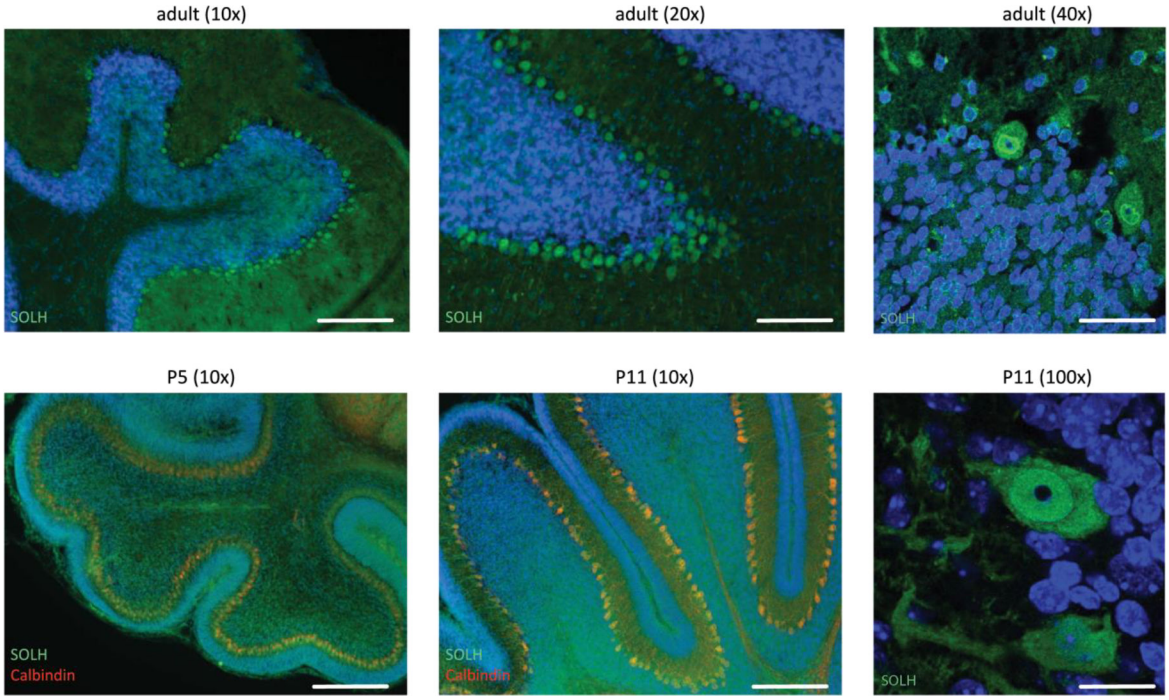


**Figure 5. Expression of CAPN15/SOLH in the maturing mouse cerebellum.**

Parasagittal images of the cerebellar hemisphere lateral to the vermis from the IV/V lobule demonstrate CAPN15 co-expression (green) with calbindin (red), a Purkinje cell marker, during early postnatal development in the mouse at timepoints critical for cerebellar maturation (postnatal day 5, bottom left; postnatal day 11, bottom middle and bottom right). Additional faint non-nuclear CAPN15/SOLH staining can be seen in the molecular layer superior to the Purkinje cells, as well as the granule zone layer inferior to the Purkinje cells. CAPN15/SOLH expression persists into the adult mouse. Scale bars as follows: top left 150 μm, top middle 75 μm, top right 37 μm, bottom left 150 μm, bottom middle 150 μm, bottom right 20 μm.

**Table 1.**

Clinical features of reported patients with *CAPN15*-related disease.

| Case series | Patient | Variant information | | | | | | Congenital abnormalities | | | | | Neurological features | | | |
|---|---|---|---|---|---|---|---|---|---|---|---|---|---|---|---|---|
| | | cDNA | Protein | Inheritance | Molecular consequence | Exon | Domain | Ocular | Cardiac | Renal | Skeletal | Sacral | ID/DD | Hearing loss | Seizure | Radiographic findings |
| Zha | 1 | NM_005632.2 c.2905G-A | p.G969S | Homozygous | Missense | 13 | SOL | × | | | | × | × | | | |
| Zha | 2 | NM_005632 c.2159C-T; c.2398C-T | p.S720F; p.R800W | Compound heterozygous | Missense; Missense | 8; 10 | CapnIIb | × | × | × | | | × | × | | |
| Zha | 3 | NM_005632.3 c.3083G-A | p.R1028K | Homozygous | Missense | 13 | SOL | × | | | | | | | | |
| Zha | 4 | NM_005632.3 c.1838C-T | p.S613L | Homozygous | Missense | 6 | CapnIIa | × | | | | × | × | × | | |
| Zha | 5 | NM_005632.3 c.1838C-T | p.S613L | Homozygous | Missense | 6 | CapnIIa | × | | | × | × | × | × | | |
| Mor-Shaked | IV-3 | NM_005632.3 c.2904+1_2905–45del | p.A913Gfs*2 | Homozygous | Exon skip | 12 | SOL | × | × | × | × | × | × | × | × | Cortical atrophy |
| Mor-Shaked | IV-7 | NM_005632.3 c.2904+1_2905–45del | p.A913Gfs*2 | Homozygous | Exon skip | 12 | SOL | × | × | × | | × | × | × | × | Cortical atrophy |
| Zaki[a] | 927-IV-2 | NM_005632.3 c.2164delC | p.R716Gfs*99 | Homozygous | Frameshift | 8 | CapnIIb | | | × | × | × | × | | | Dandy–Walker |
| Zaki[a] | 927-IV-4 | NM_005632.3 c.2164delC | p.R716Gfs*99 | Homozygous | Frameshift | 8 | CapnIIb | | | | × | | × | | | Unknown |
| Zaki[b] | 1040-IV-2 | NM_005632.3 c.754dupC | p.Q254Pfs*7 | Homozygous | Frameshift | 4 | RanBP2 | | | × | | × | | × | | Hypoplastic vermis |
| Zaki[b] | 1040-IV-4 | NM_005632.3 c.754dupC | p.Q254Pfs*7 | Homozygous | Frameshift | 4 | RanBP2 | | | × | | × | × | × | | Dandy–Walker |
| Beaman[c] | III-2 | NM_005632.3 c.2594T>C | 16p13.3del; p.L865P | Compound heterozygous | Deletion; missense | Whole gene; 11 | SOL | × | × | × | × | × | × | | | Dandy–Walker |

| Case series | Patient | Variant information | | | | | | Congenital abnormalities | | | | | Neurological features | | | |
|---|---|---|---|---|---|---|---|---|---|---|---|---|---|---|---|---|
| | | cDNA | Protein | Inheritance | Molecular consequence | Exon | Domain | Ocular | Cardiac | Renal | Skeletal | Sacral | ID/ DD | Hearing loss | Seizure | Radiographic findings |
| Beaman[c] | III-3 | NM_005632.3 c.2594T>C | 16p13.3del; p.L865P | Compound heterozygous | Deletion; missense | Whole gene; 11 | SOL | × | × | | | × | n/a | Unknown | | Dandy–Walker |

Summary of genetic, molecular, and phenotypic features of the 7 previously reported patients (described in Zha(Zha et al., 2020) and Mor- Shaked(Mor-Shaked et al., 2021) case series). Patients whose genetic information is being first reported in this paper include four whose clinical features alone were initially reported in Zaki(Zaki et al., 2015) and two previously unreported cases; all other cases presented were reported with phenotypic and genotypic information previously. (Abbreviations: CapnIIa/b, calpain protease domain; DD, developmental delay; ID, intellectual disability; RanBP2: RanBP2-motif zinc finger domain; SOL, Drosophila small optic lobes homology domain).

[c]Individual represented in Family 1 in this manuscript

Individual represented in Family 2 in this manuscript

Individual represented in Family 3 in this manuscript

**Table 2.**

Predicted binary protein interactions with CAPN15.

| Gene | Product | Function |
|---|---|---|
| *DAZP2* | DAZ-associated protein 2 | unknown |
| *HEXB* | beta hexosaminidase | lysosomal degradation of sphingolipids |
| *RN216* | ring finger nuclease 216 | NFkB pathway, E3 ubiquitin ligase |
| *TRAF2* | TNF receptor associated factor 2 | NFkB pathway, E3 ubiquitin ligase |
| *GRN* | progranulin | lysosomal membranes, regulate division of rapidly dividing cells |
| *UBQL2* | ubiquilin 2 | associates polyubiquitin chains with proteasome |

Note: Proteins predicted to have binary interactions with CAPN15 via UniProt algorithm. Notably, none of these binding partners are shared by any other calpain, suggesting that these binding partners confer unique roles to CAPN15. Proteins predicted to interact with CAPN15 have functions in ubiquitin ligation, cell division, and lysosomal processing.